Molecular Identification of Two Prophenoloxidase-Activating Proteases From the Hemocytes of Plutella xylostella (Lepidoptera: Plutellidae) and Their Transcript Abundance Changes in Response to Microbial Challenges

Authors: Shi, Min, Chen, Xiao-Yu, Zhu, Ni, and Chen, Xue-Xin

Source: Journal of Insect Science, 14(179) : 1-7

Published By: Entomological Society of America

URL: https://doi.org/10.1093/jisesa/ieu041

RESEARCH

Molecular Identification of Two Prophenoloxidase-Activating Proteases From the Hemocytes of *Plutella xylostella* (Lepidoptera: Plutellidae) and Their Transcript Abundance Changes in Response to Microbial Challenges

Min Shi, Xiao-Yu Chen, Ni Zhu, and Xue-Xin Chen[1]

Ministry of Agriculture Key Lab of Agricultural Entomology, Institute of Insect Sciences, Zhejiang University, 866 Yuhangtang Rd., Hangzhou 310058, China
[1]Corresponding author, e-mail: xxchen@zju.edu.cn

Subject Editor: Michael Kanost

J. Insect Sci. 14(179): 2014; DOI: 10.1093/jisesa/ieu041

ABSTRACT. The phenoloxidase (PO) activation system plays an important role in insect innate immunity, particularly in wound healing and pathogen defense. A key member of this system is prophenoloxidase-activating protease (PAP), which is the direct activator of prophenoloxidase (proPO). Despite their importance in the insect PO activation system, content of studies is limited. In this article, we identify two complementary DNAs (cDNAs), PxPAPa and PxPAPb, encoding possible PAPs, from immunized larval hemocytes of the diamondback moth, *Plutella xylostella* (L.), by RACE method. *PxPAPa* is 1,149-bp long and encodes a 382-residue open reading frame (ORF) with a predicted 17-residue signal peptide, a clip domain, and a Tryp_Spc domain. *PxPAPb* is 1,650-bp long and encodes a 440-residue ORF with a predicted 20-residue signal peptide, two clip domains, and a Tryp_Spc domain. PxPAPa and PxPAPb have a high sequence similarity to *Manduca sexta* (L.) PAP1 and PAP3, respectively. We also examined the transcript patterns of *PxPAPa*, *PxPAPb,* and *pxPAP3*, another clip-domain serine protease gene, response to different microbial challenges by using real-time quantitative polymerase chain reaction. The results show that the transcript abundance of PxPAPa is significantly increased by *Micrococcus luteus* and *Escherichia coli* but not *Candida albicans*. *PxPAPb* is induced only by *Mi. luteus*, whereas pxPAP3 could be induced by all the microbes in the test, but the transcript patterns of *Mi. luteus*, *E. coli*, and *C. albicans* are completely different. This study provides new insights into the molecular events that occur during the immune response, particularly melanization cascade that is involved in encapsulation and nodulation of pathogen or parasite invaders via hemocytes in host insects.

Key Words: clip-domain serine protease, immunity response, transcriptional character

Innate immunity is of great importance to insects because they lack antibodies (Iwanaga and Bok 2005). Innate immunity involves phagocytosis, encapsulation, hemocyte coagulation, and activation of the prophenoloxidase (proPO) or melanization cascade (Jiravanichpaisal et al. 2006). Activation of proPO generates phenoloxidase (PO), which catalyzes the oxygenation of monophenols to *o*-diphenols and the oxidation of *o*-diphenols to the corresponding *o*-quinones (Cerenius et al. 2008). These are reactive intermediates for melanin synthesis and other physiological processes such as cuticle sclerotization, wound healing, and pathogen sequestration (Cerenius and Söderhäll 2004). PO is synthesized in insects as an inactive zymogen, proPO, which can be activated by serine proteinases (SPs) called proPO-activating proteinase (PAP). PAPs activated via a cascade of other serine proteases in the proPO activation system are triggered by recognition of bacterial components such as peptidoglycan, β-1,3-glucan, or lipopolysaccharide (Ashida and Brey 1998, Cerenius et al. 2010).

The first PAP was identified from the cuticle of the silkworm, *Bombyx mori* L. (Dohke 1973), which was then followed by the identification of other PAPs from *Manduca sexta*, *Holotrichia diomphalia* Bates, and *Samia cynthia* Walker et Felde (Lee et al. 1998; Satoh et al. 1999; Jiang and Kanost 2000; Gupta et al. 2005; Bao et al. 2007; Kanost and Gorman, 2008). PAPs are synthesized as inactive zymogens and activated by proteolytic cleavage (Lee et al. 1998, Satoh et al. 1999). The *PAP* is constitutively expressed at high levels in the integument, whereas the transcript abundance in the fat body of naive larvae is maintained at low levels (Jiang et al. 1998, Satoh et al. 1999) but induced to higher levels in response to a bacterial challenge (Jiang et al. 1998, 2003a,b). No information on the transcript abundance in the hemocytes that circulate in the hemolymph of insect body cavity (hemocoel) is available. Also, little is known about elicitor molecules required for the induction of *PAP* transcripts.

Hemocytes are responsible for a number of defense responses in insects, including phagocytosis, nodulation, encapsulation, and melanization (Marmaras and Lampropoulou 2009). These processes appear to be discrete immune responses in terms of gene expression and outcome, but they share a number of common elements that function in concert to eliminate pathogens and parasites from the hemolymph. For example, when encapsulation (the binding of hemocytes to larger targets, such as parasites, protozoa, and nematodes) occurs, hemocytes after binding to their target form a multilayered capsule around the invader, which is ultimately accompanied by melanization. Within the capsule, the invader is killed by the local production of cytotoxic free radicals, reactive oxygen species and reactive nitrogen species, or by asphyxiation (Nappi and Ottaviani 2000).

The diamondback moth, *Plutella xylostella*, is a worldwide pest of cruciferous crops (Brassicaceae), including various important oilseed and food crops (Talekar and Shelton 1993). *P. xylostella* is the first crop pest to develop resistance to Dichloro-diphenyl-trichloroethane (DDT), and it is also the first insect to become resistant to *Bacillus thuringiensis* toxin in the field (Sarauer et al. 2003). The development of alternative pest control strategies for *P. xylostella* has typically focused on the development of insect-resistant plants and the modification of *B. thuringiensis* (Schuler et al. 2004), but researchers have recently begun to examine the use of parasitoid or parasitoid-produced regulatory molecules as environmentally safe insect control agents (Beckage and Gelman 2004). For these efforts to succeed, researchers need a more detailed understanding of host immune mechanisms. So far, the most comprehensive study of immune-related genes of *P. xylostella* is that of

Eum et al. (2007) in which the immune-inducible genes of *P. xylostella* were studied using expressed sequence tags and cDNA microarray methods. Forty-four genes were identified that were differentially expressed with at least a two-fold expression difference in *P. xylostella* before and after pathogen challenge, whereas another 70 genes were identified as candidate immune response genes, but none of them was *PAP* genes.

In this study, we cloned two cDNAs encoding PAP from hemocytes of immunized *P. xylostella* larvae and studied their elicitor specificity in hemocytes. All the results will provide new insights into the molecular events that occur during the immune response to pathogens or parasites in *P. xylostella*.

Materials and Methods

Insect and Microbes. Pupae of *P. xylostella* were initially collected from cabbage in the suburbs of Hangzhou, Zhejiang province, China. The resulting larvae were reared at 24°C, 65% relative humidity (RH), and 14: 10 (L:D) h and fed on a diet of cabbage. Moths were fed with a 20% (v/v) honey/water solution. Microbes used in experiments were *Escherichia coli* (Gram negative, G^-) (strain: DH5α, TaKaRa, Dalian, China), *Micrococcus luteus* (Gram positive, G^+) (CICC 10209, China Center of Industrial Culture Collection), and *Candida albicans* (fungus, F) (ATCC 10231, American Type Culture Collection).

Total RNA Isolation and First-Strand cDNA Synthesis. *E. coli*, *Mi. luteus*, and *C. albicans* were cultured overnight in 5 ml of Luria–Bertani medium, nutrient broth medium, and Martin broth (modified) medium, respectively, at 30°C in a rotating incubator. Before injection, the bacterial and fungal samples were killed by boiling in water for 5 or 20 min, respectively, and then the microbes were suspended in phosphate buffered saline (PBS) for injection. Fourth-instar larvae (feeding stage) were each injected with 0.2 µl of sterilized phosphate buffered saline (PBS, pH 6.8), heat-killed *E. coli* (1×10^4 cells per larva), *Mi. luteus* (1×10^4 cells per larva), or *C. albicans* (1×10^4 cells per larva) with a glass needle mounted on a NN-153 type micromanipulator (Narishigen, Tokyo, Japan), respectively. PBS was used as a control. Hemocyte samples for each experimental group were collected from at least 30 *P. xylostella* larvae at 1, 2, 4, 8, 12, and 24 h post injection (h.p.i.). Hemocytes were collected by bleeding larvae from a cut proleg into PBS buffer and pelleting the cells by gentle centrifugation ($400 \times g$ for 1 min). All collected samples were immediately used for the isolation of total RNA using High Pure RNA Isolation kit (Roche, Manneheim, Germany) according to the manufacturer's instructions, and then RNA was quantified using a Nanodrop spectrometer 1000 (NanoDrop Technologies, Rockland, DE).

For the first-strand cDNA synthesis, 1 µg of total RNA was reverse transcribed in 20-µl reactions by using random hexamers and Superscript III Reverse Transcriptase (Invitrogen, Shanghai, China). Real-time polymerase chain reactions (RT-PCRs) were run using an Eppendorf thermocycler (Eppendorf, Hamburg, Germany) and 25 µl of reaction volumes containing 1 µl of cDNA and 2.5 mM of appropriate gene-specific primers.

Cloning and Sequencing PxPAP cDNAs. Messenger RNA (mRNA) was purified from the total RNA using a QuickPrep Micro mRNA Purification Kit (Pharmacia, Stockholm, Sweden). The cDNA fragments of *PxPAPs* were obtained by degenerate primers (Table 1) designed from the conserved region of the SP domain of PAPs using the available sequences of insect PAP genes in GenBank. Primers PAP-degenerate-F and PAP-degenerate-R (Table 1), designed from the conserved amino acid sequences IDQYPW and GDSGGP, respectively, were used for PCR amplification.

The first-strand cDNAs of hemocyte samples were used as templates in a 25 -µl PCR reaction containing the primer pair PAP-sp-F and PAP-sp-R (0.2 mM each), dNTP (10 mM), PCR buffer (1X), and Taq DNA polymerase (1.0 U). The PCR conditions consisted of an initial denaturation at 94°C for 3 min, followed by 35 cycles of denaturation at 94°C for 1 min, annealing at 55°C for 1 min, extension at 72°C for 1 min, and a final extension at 72°C for 10 min. The PCR product was analyzed by 1.5% agarose gel electrophoresis, and the PCR product of the expected molecular size (600 bp) was removed from the gel and cloned into the pGEM-T Easy vector (Promega, Madison, WI).

The *PxPAP* gene-specific primers (Table 1) were designed to amplify the full cDNA sequences by using 5′-Full Race Kit and 3′-Full Race Kit (TaKaRa, Dalian, China), and full open reading frames (ORFs) of *PxPAP* were verified by PCR reaction. Amplified fragments were purified using the QIAquick Gel Extraction Kit (Qiagen, Hilden, Germany) and ligated directly into the pGEM-T Easy Vector (Promega, Madison, WI). The positive clones were first screened using blue and white colony screening method, and then positive clones were tested

Table 1. Sequences of primers used in this study

Primer name	Sequence (5′→3′)	Used for
PAP-degenerate-F	ATCGAYCARTAYCCNTGG	Degenerate PCR
PAP-degenerate-R	CATGAGSGGRCCRCCSGA	Degenerate PCR
PxPAPa-sp-3r-outer	CAAGTCCAGTGAAAACCAAGCTCGG	3′-RACE
PxPAPa-sp-3r-inner	TGTTCGCCCAAGACGCCTGT	3′-RACE
PxPAPa-sp-5r-outer	ATCCAGTCTTTGTAGGAGGCCACG	5′-RACE
PxPAPa-sp-5r-inner	CTCCGTCTGGTCTCCTCTTCATC	5′-RACE
PxPAPa-orf-F	ATCATCGCATTTATCACCTCAA	ORF verified, construct plasmid
PxPAPa-orf-R	AAACGAAACATCCATTATCCCT	ORF verified, construct plasmid
PxPAPa-rt-F	CTCAAGAGATAGCAGTGGACCG	RT-qPCR
PxPAPa-rt-R	TGTGCCATTCTGACTAGAGCGA	RT-qPCR
PxPAPb-sp-3r-outer	AGACAGGAACAGCGAGTG	3′-RACE
PxPAPb-sp-3r-inner	CTCCCAGGGCAATAGG	3′-RACE
PxPAPb-sp-5r-outer	GTCCTTGCCTTGCCCTTCAGT	5′-RACE
PxPAPb-sp-5r-inner	GGCGGCTGTCAGAGCGTATTT	5′-RACE
PxPAPb-orf-F	ATGGAAAAGTGACCGAGCGAA	ORF verified, construct plasmid
PxPAPb-orf-R	TCACTACCACAACTATTCTCA	ORF verified, construct plasmid
PxPAPb-rt-F	TACGACAAGAGCAACGACGG	RT-qPCR
PxPAPb-rt-R	TCGGATGTGGTATGGACTTCT	RT-qPCR
pxPAP3-orf-F	TATGTGGAGGTGACAGTTCA	ORF verified, construct plasmid
pxPAP3-orf-R	CTGACGACACCGACCACAAT	ORF verified, construct plasmid
pxPAP3-rt-F	CCTTTCGTCCATCCATCCTT	RT-qPCR
pxPAP3-rt-R	CTATGTTGCCACCGATAATCC	RT-qPCR
Pxβ-actin-F	GGAGTGATGGTCGGTATGGG	PCR, construct plasmid
Pxβ-actin-R	CATGAGGTAGTCGGTCAAGTCG	PCR, construct plasmid
Pxβ-actin-rt-F	TGGCACCACACCTTCTAC	RT-qPCR
Pxβ-actin-rt-R	CATGATCTGGGTCATCTTCT	RT-qPCR

again with degenerate primers to reduce the number of false positive clones.

The recombinant plasmids were isolated from cultured *E. coli* cells by an alkaline miniprep method. The presence of the insert was verified by PCR amplification with M13 forward and reward sequencing primers, and then sequenced (Invitrogen, Shanghai, China) on both strands to obtain the complete consensus sequence.

Sequence Analysis and Phylogenetic Reconstruction. *PxPAPs* and deduced amino acid sequences were analyzed using DNASTAR programs (version 5.02) (DNASTAR, Inc., Madison, WI). Signal peptide and domain prediction were performed by SMART (http://smart.embl-heidelberg.de/). Translation of *PxPAPs* and prediction of the deduced proteins were conducted with ExPASy (http://www.au.expasy.org/). Homologous protein sequence comparisons with entries in the updated GenBank/EMBL, SWISS-PROT, and PIR databases were performed with Blast and PSI-Blast programs with an *E*-value cut-off of 10^{-8} (Friedman and Hughes 2006). Sequence alignment was performed with ClustalX version 1.81 using default parameters (Thompson et al. 1997) and edited using GeneDoc (version 2.04) (Free Software Foundation, Inc., MA). Maximum parsimony (MP) method was used for phylogenetic analysis with Mega 5.1 (Kumar et al. 2008), and bootstrap analysis provided support values for the branches (Felsenstein 1985). Clip domain, catalytic residues, and substrate-specific residues of PxPAPs were predicted through a multiple alignment of homologous sequences.

RT-Quantitative PCR. RT-quantitative PCR (RT-qPCR) was performed to further compare transcript abundances of PxPAPs in the larval hemocytes after exposure to microbial challenges. Total RNA was isolated from the hemocytes of *E. coli* (G^+), *Mi. luteus* (G^-), and *C. albicans* (F) injected larvae, using High Pure RNA Isolation kit (Roche, Manneheim, Germany) according to the manufacturer's instructions. Quantification of RNA was done using a Nanodrop spectrometer 1000 (NanoDrop Technologies, Roackland, DE).

RT-qPCR reactions were run on an Eco Thermal Cycler (Illumina, San Diego, CA) in 10-µl reactions. Each 10-µl reaction contained 1 µl of template cDNA, 5 µl of THUNDERBIRD SYBR qPCR Mix (TOYOBO, Osaka, Japan), and 0.5 µM each of the corresponding forward and reverse primers. Primer pairs used for RT-qPCR experiments were designed from ORF sequences of *PxPAPs* (Table 1). To normalize differences in total RNA amounts that were reverse transcribed and added to each reaction, *β-actin* from *P. xylostella* (*Pxβ-actin*) (GenBank JN410820) was used as an active endogenous control. Based on T_m value of primer pairs, cycling conditions were designed as follows: 1 min initial denaturation step at 95°C, followed by 40 cycles of 15 s denaturation at 95°C, 35 s annealing at 60°C, then one cycle of 15 s at 95°C, 15 s at 60°C, and 15 s at 95°C to produce the melting curves data. Data were acquired during the extension step and analyzed with the Eco Real-Time PCR detection system. Each amplification reaction was carried out in three biological replicates from which *PxPAPs* mean threshold cycle (C_T) values plus standard deviations were calculated. Relative transcripts of *PxPAPs* were calculated using the $2^{-\Delta\Delta CT}$ method (Livak and Schmittgen 2001). To validate the use of the $2^{-\Delta\Delta Ct}$ method, the amplification efficiency of *PxPAP* gene-specific primers were calculated. The plasmid pGEM-T, which contains full ORF sequences of *PxPAPs* or 450 bp fragment of *Pxβ-actin*, was diluted 10-fold in PBS buffer with 10^1–10^5 copies per reaction. Each amplification reaction was carried out in three replicates, and the corresponding R^2 values of standard curves were calculated. Amplification efficiency (E) of semiquantitative RT-qPCR was determined based on slope values obtained from linear regressions, where C_t values were plotted versus the logarithmic values of serially diluted input plasmid DNA templates by employing the equation $E = 10^{(-1/\text{Slope})} - 1$ (Peirson et al. 2003). Amplification efficiencies of targets and endogenous controls were also calculated and compared to ensure that the corresponding amplicons were amplified at similar rates over a certain dynamic range. To compare transcript abundance for a given gene among time points, we calibrated each ΔC_t value against the 1 h post-PBS injection samples, generating a $\Delta\Delta C_t$ value, followed by transformation using the expression $2^{-\Delta\Delta Ct}$ to obtain relative transcript abundance values (RA), which were nonnormally distributed.

Statistical Analysis. The transcript abundances of *PxPAPs* were analyzed using one-way analysis of variance (ANOVA). The differences in the transcripts of *PxPAPs* were compared using Dunnett's multiple comparison and Least Significant Difference (LSD) comparison post hoc tests. All statistics were performed using the SPSS software (SPSS 16.0, SPSS Inc., Chicago, IL).

Results

Complete cDNAs of PxPAP Genes. We designed two degenerate primers based on the highly conserved amino acid sequence of PAPs of Lepidoptera in the database. Using these primers, we got two fragments, which had sizes of ~600 bp. These bands were removed and subcloned into pGEM-T Easy vector. Then we sent 10 positive clones for each fragment to Invitrogen Biotechnology Company (Invitrogen, Shanghai, China) for sequencing. In all, 40 clones were sequenced along with four clones for partial PxPAPa and five clones for partial PxPAPb. Using RACE technique and *PxPAPs* gene-specific primers based on verified fragment sequences of PxPAPa and PxPAPb, we obtained the full-coding cDNA sequences of *PxPAPa* and *PxPAPb*.

The full-length cDNA of *PxPAPa* (1,595-bp long, GenBank JQ581597) (Fig. 1A) contained a 5′-untranslated region (UTR) of 196 bp, a 3′-UTR of 250 bp, and an ORF of 1,149 bp encoding a putative PAP protein of 382 amino acids with deduced molecular weight (MW) of 41.31 kDa and theoretical isoelectric point (*p*I) of 7.78. The full-length cDNA of *PxPAPb* (1,650 bp long, GenBank JQ581598) (Fig. 1B) contained a 5′-UTR of 125 bp, a 3′-UTR of 201 bp, and an ORF of 1,323 bp encoding a putative PAP protein of 440 amino acids with deduced MW of 47.89 kDa and theoretical *p*I of 7.04.

Assembled cDNA sequences of pxPAPs revealed that sequences of 3 positive clones of amplified fragments were identical to the sequence of one complete mRNA in GenBank with 100% (GenBank AB282644). As the authors annotated that it was "*Plutella xylostella PxPAP 3* mRNA for PxProphenoloxidase-activating proteinase 3," we accepted that it was one *PAP* gene of *P. xylostella* and named as *pxPAP3*. Because it is only published in the database with no additional functional analysis, we continued to describe and analyze the molecular characters of pxPAP3. The full-length cDNA of *pxPAP3* (1,786 bp) (Fig. 1C) contained a 5′-UTR of 81 bp, a 3′-UTR of 445 bp, and an ORF of 1,260 bp encoding a putative PAP protein of 420 amino acids with deduced MW of 45.71 kDa and theoretical *p*I of 6.18.

Amino Acid Sequences of PxPAP Proteins and Phylogenetic Analysis. The first 17 amino acid sequences of PxPAPa (Fig. 1A) were predicted as the signal peptide. A typical clip domain was located between amino acids from 20 aa to 73 aa, and the conserved Trypsin-like serine protease (Tryp_Spc) catalytic triad domain was found between amino acids from 126 to 373 aa. According to NetNGlyc and NetOGlyc programs, there are 6 potential N-linked and 12 potential O-linked glycosylation sites present in the sequence of PxPAPa. Further amino acid sequence analysis revealed that PxPAPa has the common structural features of the clip-domain serine proteinase (clip-SP) family with the highly conserved six cysteine residues in the N-terminal clip domain, which could form three pairs of disulfide bonds (Cys1-Cys5, Cys2-Cys4, Cys3-Cys6), the three conserved His-Asp-Ser catalytic triad residues (His^{172}, Asp^{234}, Ser^{329}) located in three patterns of conserved sequence, TAAHC, DIAL, and GDSGGP, respectively, at the C-terminal serine proteinase domain, with a short link sequence between these two domains. The PxPAPa clip domain has a calculated MW of 5.85 kDa and a *p*I of 7.64, and the Tryp_Spc domain is 26.96 kDa and 7.81, respectively. The predicated site for proteolytic activation is between Arg^{126} and Ile^{127}. The primary substrate-specificity pocket is likely composed of Asp^{323}, Gly^{351}, and Gly^{361} Additionally, the residue number between Cys3 and Cys4 of PxPAPa clip domain was 24. Also, a signature motif composed of two

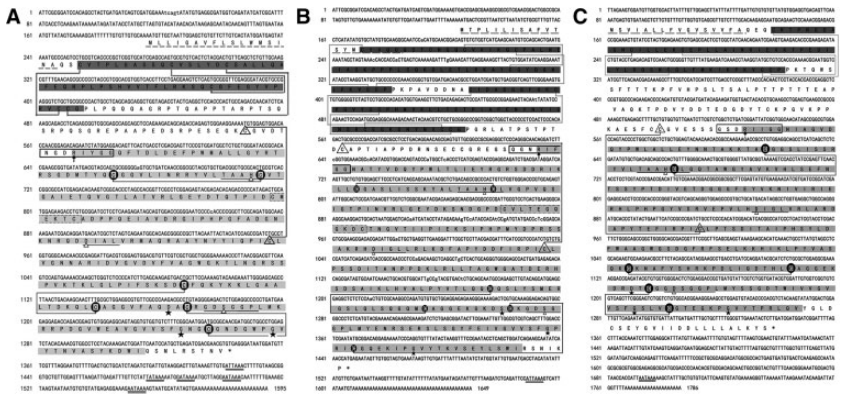

Fig. 1. Nucleotide sequence of and deduced amino acid sequence of the ORFs of *PxPAPa* (A), *PxPAPb* (B), and *pxPAP3* (C) cDNA. Polyadenylation signals were double underlined. Signal peptide is dash underlined. The active region is open boxed, and arrow indicated the active site. Clip domain is gray covered, and conserved three pairs of cysteine residues disulfide bridges were showed by gray lines. Tryp_Spc domain is light gray covered. Conserved catalytic motifs were underlined by black lines, and catalytic triad sites were marked by open triangles. The substrate specificity sites were marked by dark stars. Cysteine residues of Tryp_Spc domain and corresponded disulfide bridges were marked by closed black circles and showed by the black lines, respectively. Two cysteine residues of interdomain and corresponded disulfide bridge were open triangle boxed and showed by black line, respectively. The PAP signature loop was dotted line boxed.

cysteine residues was found at positions 201 aa and 206 aa, following a conserved sequence "VRLGEYD."

PxPAPb (Fig. 1B) has a signal peptide, two clip domains, and a Tryp_Spc domain, and they are located at the region between 1–20 aa, 16–72 aa, 82–134 aa, and 156–420 aa, respectively. NetNGlyc and NetOGlyc programs indicate there are two potential N-linked glycosylation and three potential O-linked glycosylation sites present in the amino acid sequence of PxPAPb. Further amino acid sequence analysis reveals that the residue numbers between Cys3 and Cys4 of PxPAPb clip domain are 25 and 24, respectively, and the three conserved His-Asp-Ser catalytic triad residues of Tryp_Spc domain (170–434 aa) are composed of His^{217}, Asp^{284}, and Ser^{384}. The calculated MW of dual PxPAPb clip domains and the Tryp_Spc domain are 6.19, 5.86, and 28.81 kDa, respectively, and the corresponding *p*Is are 8.19, 4.85 and 6.79, respectively. The predicated site for proteolytic activation is between Arg^{170} and Ile^{171}. The primary substrate-specificity pocket is likely composed of Asp^{379}, Gly^{411}, and Gly^{422}. Again, the same signature motif composed of two cysteine residues was found at positions 246 aa and 256 aa, following a conserved sequence "VRLGEYD."

pxPAP3 (Fig. 1C) has a signal peptide, a clip domain, and a Tryp_Spc domain, and they are located at the region between 1–16 aa, 20–74 aa, and 150–396 aa, respectively. NetNGlyc and NetOGlyc programs suggest that there are 2 potential N-linked glycosylation and 13 potential O-linked glycosylation sites present in the amino acid sequence of pxPAP3. Further amino acid sequence analysis revealed that the residue numbers between Cys3 and Cys4 of pxPAP3 clip domain is 36, and the three conserved His-Asp-Ser catalytic triad residues of Tryp_Spc domain is composed of His^{194}, Asp^{258}, and Ser^{356}. pxPAP3 clip domains have the calculated MW of 6.16 kDa and a *p*I of 8.0, and the Tryp_Spc domain is 27.05 and 7.37 kDa, respectively. The predicated site for proteolytic activation is between Arg^{150} and Ile^{151}. The primary substrate-specificity pocket is likely composed of Asp^{350}, Gly^{377}, and Gly^{388}. In contrast to PxPAPa and PxPAPb, we do not find the signature motif composed of two cysteine residues before conserved sequence "VRLGEXD" in the amino acid sequence of pxPAP3.

Homologs of PxPAPs were found among lepidopteran species by PSI-BlastP. These homologs had different lengths of amino acids ranging from 371 aa to 455 aa. PxPAPa had the highest identity, up to 68%, with the sequence of HaPAE, whereas PxPAPb had the highest identity, up to 51%, with the sequence of MsPAP3. The topology of the MP tree (Fig. 2) generated by Mega 5.1 shows that all the homologous sequences comprised two groups with PxPAPa, PxSP7, BbPAP1, MsPAP1, HaPAE, SlPAE1, and MsHP8 clustered into the first group and the rest

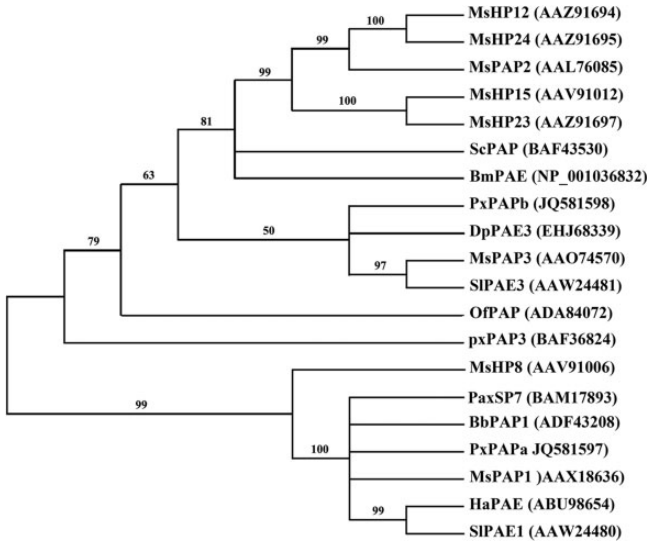

Fig. 2. Phylogenetic analyses of PxPAPs. Maximum parsimony tree was generated using Mega 5.1 from the alignment of the homologous protein sequences retrieved by PSI-BlastP analysis. Taxa name was composed of abbreviation of species name, gene name, and sequence GenBank accession number. Ms, *Manduca sexta*; Sc, *Samia Cynthia*; Bm, *Bombyx mori*; Dp, *Danaus plexippus*; Sl, *Spodoptera litura*; Of, *Ostrinia furnacalis*; Pax, *Papilio xuthus*; Bb, *Biston betularia*; and Ha, *Helicoverpa armigera*. Numbers at nodes were bootstrap values (%).

in the second group. In the second group, we found two obvious subgroups, the first including DpPAP3, PxPAPb, MsPAP3 and SlPAE3, pxPAP3, and OfPAP, and the second including MsHP24, MsHP12, MsPAP2, MsHP15, MsHP23, BmPAE, and ScPAP.

Transcript Abundance of PxPAP and pxPAP3 Response to Microbial Challenges. We used RT-qPCR and time course experiments to compare the relative abundance of PxPAPs in hemocytes of microbial challenged larvae. The R^2 values of a standard curve of PxPAPa, PxPAPb, pxPAP3, and Pxß-actin were 0.9882, 0.9965, 0.9966, and 0.9986, and amplification efficiencies (E) of 104.3, 107.6, 107.9, and 109.2%. Additionally, the C_t values of the internal control, *Pxß-actin*, did not differ between time points (ANOVA, $df = 5$, $F = 2.95$, $P = 0.058$).

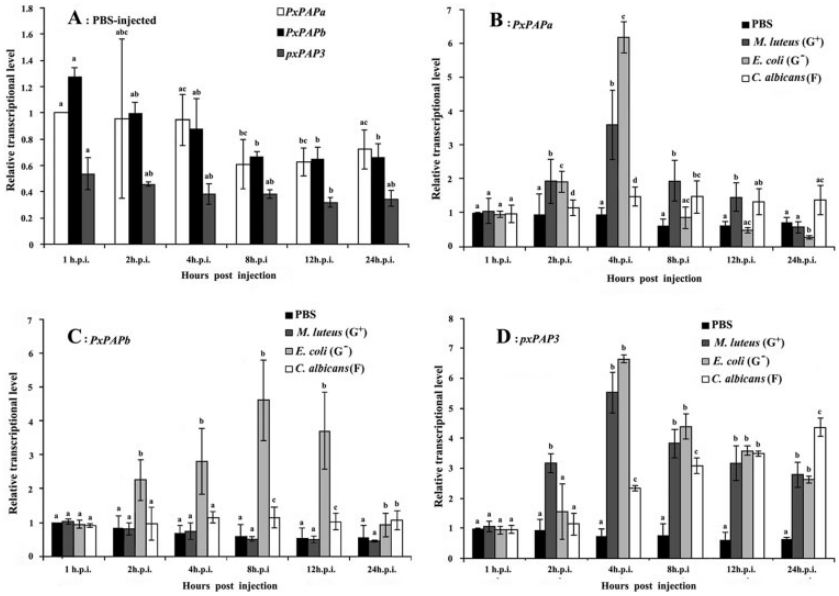

Fig. 3. RT-qPCR analyses of *PxPAPs* and *pxPAP3* transcript levels in hemocytes. (A) RT-qPCR analysis of *PxPAPs* transcript abundance in hemocytes from larvae injected with PBS. (B–D) RT-qPCR analysis of the transcript abundance of *PxPAPa*, *PxPAPb*, and *pxPAP3*, respectively, in hemocytes from larvae injected with heat-killed microbes. Transcript abundance was measured in each sample at 1, 2, 4, 8, 12, and 24 h postinjection. Each treatment and time point were measured three times by using independently collected samples. (A) Different letters above a given bar indicate that they significantly differ from the transcript abundance of one given *PxPAP* gene within the different time point post PBS injection (ANOVA test, $P < 0.05$). (B–C) Different letters above a given bar indicate that they significantly differ within transcript abundance of *PxPAPa*, *PxPAPb*, or *pxPAP3* in response to different microbial challenges at one given time point post injection (ANOVA test, $P < 0.05$), respectively. Error bars ± SEM.

We noticed that the injection of PBS alone also caused the transcript levels to change (Fig. 3A). When we standardized the transcript levels of *PxPAPa* at 1 h.p.i. to a value of 1, we found that *PxPAPb* had the highest transcript level among three genes, whereas the *pxPAP3* has the lowest transcript level. As RT-qPCR results showed there was a small transcriptional peak of three genes at 1 h.p.i., shortly after PBS was injected, then the transcript abundance of *PxPAPb* and *pxPAP3* declined to a stable level, while the transcript level of *PxPAPa* began to decline at 4 h.p.i.. However, the induced transcripts level of *pxPAP3* by PBS injection was apparently much lower than those of *PxPAPa* and *PxPAPb*.

We next compared how transcript abundance of *PxPAPa* and *PxPAPb* was affected by different immune challenges. For convenience, first, we standardized the transcript levels of each of the *PxPAP* genes of 1 h post-PBS injected to a value of 1. As shown in Fig. 3B and C, for each *PxPAP* gene, differences between its transcript levels existed when the larva was injected with different types of microbes, i.e., *E. coli* (G^-), *Mi. luteus* (G^+), and *C. albicans* (F).

Compared with injection of PBS only, the injection of *E. coli* (G^-) and *Mi. luteus* (G^+) induced significantly higher transcript abundance of *PxPAPa*, whereas the injection of *C. albicans* (F) induced slightly higher transcript abundance (Fig. 3B). The transcript patterns of *PxPAPa* in response to each microbe injection were similar but different from controls. Additionally, after injection of *E. coli* (G^-) and *Mi. luteus* (G^+), the transcript level of *PxPAPa* greatly increased to a maximum at 4 h.p.i., then quickly declined. However, after injection of *C. albicans* (F), the transcript abundance of *PxPAPa* just slightly and slowly increased to the maximum at 4 h.p.i., and then was stable at later time points. The maximal transcript level of *PxPAPa* in response to injection of *Mi. luteus* was 1.72-fold and 4.18-fold of those in response to injection of *E. coli* (G^-) and *C. albicans* (F), which suggested the transcript abundance of *PxPAPa* might be significantly induced by bacteria, whether it was *E. coli* (G^-) or *Mi. luteus* (G^+).

Compared with controls, only the injection of *E. coli* (G^-) significantly increased the transcript abundance of *PxPAPb*, whereas injection of *Mi. luteus* (G^+) or *C. albicans* (F) had no effect (Fig. 3C), which suggests the transcript abundance of *PxPAPb* is induced by *E. coli* (G^-). The transcript patterns of *PxPAPb* in response to injection of *E. coli* (G^-) and *C. albicans* (F) were different from that in response to injection of *Mi. luteus* (G^+), which was similar to controls. The transcript abundance of *PxPAPb* in response to injection of *E. coli* (G^-) increased to the maximum at 8 h.p.i., whereas the transcript abundance of *PxPAPb* in response to injection of *C. albicans* (F) increased to the maximum at 4 h.p.i. The maximum transcript abundance of *PxPAPb* after injection of *E. coli* (G^-) was 3.98-fold as compared with *C. albicans* (F). The transcript abundance of *PxPAPb* in response to injection of *Mi. luteus* (G^+) steadily declined over 24 h, similar to controls.

The injection of all three microbes significantly induced the transcript abundance of *pxPAP3*, but transcript patterns of *pxPAP3* in response to bacteria and fungus injections were different from each other (Fig. 3D) and from controls. At 4 h.p.i. of *E. coli* (G^-) and *Mi. luteus* (G^+), the transcript abundance of *pxPAP3* increased to its maximum and then declined. In contrast, after the injection of *C. albicans* (F), the transcript abundance of *pxPAP3* steadily increased over 24 h. The maximum transcript abundance of *PxPAPb* in response to injection of *Mi. luteus* (G^+) was 1.2-fold and 1.5-fold of those in response to injection of *E. coli* (G^-) and *C. albicans* (F), which suggested the transcript abundance of *pxPAP3* was induced at similar levels by all three microbes, regardless of species.

Discussion

The significance of proPO activation in insect physiology and immunity has been appreciated for many years, and molecular and biochemical characterization of proteinase-activating proPO only has been reported in limited insect systems. The predicted proteins of PxPAPa and PxPAPb, we cloned from *P. xylostella*, and pxPAP3, a former identified cDNA, show the characteristics of the clip-SPs (Jiang and Kanost 2000). The trypsin-like specificity pocket, Asp-Gly-Gly, which is consistent with the specificity of PAPs that cut at Arg*Phe, suggested a possible role as the PAP (Jiang and Kanost 2000). Additionally, the clip

domain of PxPAPa, PxPAPb, and pxPAP3 all belong to group 2 clip domains (Iwanaga et al. 1998). Different to pxPAP3, the existence of a signature motif in catalytic domain indicated PxPAPa and PxPAPb are real PAPs (Jiang and Kanost 2000, Ross et al. 2003).

The results of our phylogenetic analysis clearly grouped PxPAPa with MsPAP1 and grouped PxPAPb with MsPAP3. The domain organization of PxPAPa (one clip domain and a catalytic SP domain) and PxPAPb (two clip domain and a catalytic SP domain) supported the PxPAPa was corresponding to PAP1 in *M. sexta*, and PxPAPb was corresponding to PAP3. Most of the homologous proteins we found in database by Blast search were part of the large-scale sequencing project and had not been characterized functionally. We only can suppose that pxPAP3, locating in the base place of PAP1 group in phylogenetic tree, is one of the proteins which involved in a proteinase pathway that generates active PO for melanin production (Cerenius and Söderhäll 2004), such as proPO-activating factors.

So far, our knowledge of the transcriptional regulation of the insect proPO activation system is largely limited to proPO, which appear to be transcriptionally unresponsive to pathogen or parasite infection. For instance, Dimopoulos et al. (1997) found that mRNA levels of six *Anopheles gambiae* proPO did not significantly change after a bacterial challenge. There might be many factors contributing to this unresponsive character of proPO (Zou et al. 2005). Activation of proPO cascade components after immune invasion is a reasonable way to control activation of PO. The activation of PAPs is the most immediate part of immune response in insect, and it will happen in minutes post immune invasion. The expression of PAPs or the transcript abundances of *PAPs* were already reported to be upregulated in fat body by the injection of microbes and their cell wall components (Jiang et al. 1998, 2003a,b, 2011; Gorman et al. 2000; De Gregorio et al. 2001; Bao et al. 2007). However, it is not clear that, in hemocytes, there is any difference among the transcript abundances of a given *PAP* gene corresponding to the challenge of negative Gram bacteria, positive Gram bacteria, and fungus, respectively.

Some hemocyte-generated insect immune-related molecules, like antimicrobial peptides, have no significant transcriptional response to a simple wound from a needle. For example, in *Pseudoplusia includens* Walker, Lavine et al. (2005) found that the simple injection with a sterile glass needle resulted in the transcript abundances of three antimicrobial peptide genes in hemocytes that were only slightly higher than those of control larvae. However, the proPAP activation cascade components are different. A simple wounding can cause the activation of proPO, and once be activated, PO activity localizes to the wound sites, which limits global melanization of hemolymph. In this study, to exclude the effect from wounding of injecting needle and the injection of PBS buffer, we used RNA samples from PBS-injected *P. xylostella* larvae as negative control in the RT-qPCR. Before we used RT-qPCR method to examine the transcript abundances of *PxPAPa*, *PxPAPb*, and *pxPAP3* in response to immune challenges from three different types of microbes, i.e., *E. coli* (G^+), *Mi. luteus* (G^-) and *C. albicans* (F). We first examined the transcript abundance of *PxPAPa*, *PxPAPb*, and *pxPAP3* in response to injection of PBS buffer with sterile microinjection needle. Our result showed that the wound from simple injection would cause a small amount of up-regulated transcript of *PxPAPa* and *PxPAPb* but not so obviously of *pxPAP3*. It suggested that PxPAPa and PxPAPb might be involved in the local proPO activation in response to the wound, but pxPAP3 was not.

The differences among the transcript abundance changes of *PxPAPa*, *PxPAPb*, and *PxPAP3* when the larvae were injected with *E. coli* (G^-), *Mi. luteus* (G^+), and *C. albicans* (F), respectively, indicated the following: 1) the transcript abundance of *PxPAPa* was majorly induced by bacteria, whatever it was Gram negative or positive; 2) the transcript abundance of *PxPAPb* was majorly in response to *E. coli* (G^-); and 3) the transcript abundance of *pxPAP3* had significant responses to all three test types of microbes but their patterns of transcript abundance were different.

In this study, we show the important differences in transcript patterns of PAP genes in hemocytes of *P. xylostella* when they faced different immune-challenging microbes, which give us some ideas about the biological and functional cascade of different *PAP* genes during proPO activation and melanization which is involved in the encapsulation and nodulation of different pathogen or parasite invaders via hemocytes in *P. xylostella*. However, why such difference in transcript abundance of a given PAP gene exist and how the transcriptional regulation of a given PAP gene is related to different types of microbes remained largely unknown, which are worthy of the future study.

Acknowledgments

We thank Dr. M. R. Strand (University of Georgia) for his help in manuscript writing. This study was supported jointly by the 973 Program of China (2013CB127603), Zhejiang Provincial Natural Science Foundation of China (Z3100296), and Zhejiang Key Program of Agriculture of China (2009C12048) to X.-X.C., and the National Science Foundation of China (30971907) and the Zhejiang Science Fund for Distinguished Young Scholars of China (R3110049) to M.S.

References Cited

Ashida, M., and P. Brey. 1998. Recent advances in research on the insect prophenoloxidase cascade, pp. 135-172. *In* **P. T. Brey and D. Hultmark** (eds.), Molecular mechanisms of immune responses in insects. Chapman and Hall, London, United Kingdom.

Bao, Y., Y. Yamano, and I. Morishima. 2007. β-1,3-Glucan inducible expression of prophenoloxidase-activating proteinase from eri-silkworm, Samia cynthia ricini. Comp. Biochem. Physiol. 147: 45-48.

Beckage, N. E., and D. B. Gelman. 2004. Wasp parasitoid disruption of host development: implications for new biologically based strategies for insect control. Ann. Rev. Entomol. 49: 299–330.

Cerenius, L., and K. Söderhäll. 2004. The prophenoloxidase-activating system in invertebrates. Immunol. Rev. 198**:** 116–126.

Cerenius, L., B. L. Lee, and K. Söderhall. 2008. The proPO-system: pros and cons for its role in invertebrate immunity. Trends Immunol. 29: 263–271.

Cerenius, L., S. I. Kawabata, B. L. Lee, M. Nonaka, and K. Söderhäll. 2010. Proteolytic cascades and their involvement in invertebrate immunity. Trends Biochem. Sci. 35: 575–583.

De Gregorio, E., P. T. Spellman, G. M. Rubin, and B. Lemaitre. 2001. Genome-wide analysis of the *Drosophila* immune response by using oligonucleotide microarrays. Proc. Natl Acad. Sci. U S A. 98: 12590–12595.

Dimopoulos, G., A. Richman, H. M. Muller, and F. C. Kafatos. 1997. Molecular immune response of the mosquito *Anopheles gambiae* to bacteria and malaria parasites. Proc. Natl Acad. Sci. U S A. 94: 11508–11513.

Dohke, K. 1973. Studies on prophenoloxidase-activating enzyme from cuticle of the silkworm, *Bombyx mori*. II. Purification and characterization of the enzyme. Arch. Biochem. Biophys. 157: 210–221.

Eum, J. H., Y. R. Seo, S. M. Yoe, S. W. Kang, and S. S. Han. 2007. Analysis of the immune-inducible genes of *Plutella xylostella* using expressed sequence tags and cDNA microarray. Dev. Comp. Immunol. 31: 1107–1120.

Felsenstein, J. 1985. Confidence limits on phylogenies: An approach using the bootstrap. Evolution 39: 783–791.

Gorman, M. J., O. V. Andreeva, and S. M. Paskewitz. 2000. Molecular characterization of five serine protease genes cloned from *Anopheles gambiae* hemolymph. Insect Biochem. Mol. Biol. 30: 35–46.

Gupta, S., Y. Wang, and H. Jiang. 2005. Purification and characterization of *Manduca sexta* prophenoloxidase-activating proteinase-1 (PAP-1), an enzyme involved in insect immune responses. Protein Expr. Purif. 39: 261–268.

Iwanaga, S., and L. L. Bok. 2005. Recent advances in the innate immunity of invertebrate animals. J. Biochem. Mol. Biol. 38: 128–150.

Iwanaga, S., S. Kawabata, and T. Muta. 1998. New types of clotting factors and defense molecules in hosrshoe crab hemolymph: their structures and functions. J. Biochem. 123: 1–15.

Jiang, H., and M. R. Kanost. 2000. The clip-domain family of serine proteinases in arthropods. Insect Biochem. Mol. Biol. 30: 95–105.

Jiang, H., Y. Wang, and M. R. Kanost. 1998. Pro-phenol oxidase activating proteinase from an insect, *Manduca sexta*: a bacteria-inducible protein similar to *Drosophila* easter. Proc. Natl Acad. Sci. U S A. 95: 12220–12225.

Jiang, H., Y. Wang, X. Q. Yu, and M. R. Kanost. 2003a. Prophenoloxidase-activating proteinase-2 from hemolymph of *Manduca sexta*: a bacteria-inducible serine proteinase containing two clip domains. J. Biol. Chem. 278: 3552–3561.

Jiang, H., Y. Wang, X. Q. Yu, Y. Zhu, and M. Kanost. 2003b. Prophenoloxidase-activating proteinase-3 (PAP-3) from *Manduca sexta* hemolymph: a clip-domain serine proteinase regulated by serpin-1J and serine proteinase homologs. Insect Biochem. Mol. Biol. 33: 1049–1060.

Jiang, H. B., A. Vilcinskas, and M. R. Kanost. 2011. Immunity in Lepidopteran insect. Adv. Exp. Med. Biol. 708: 181–205.

Jiravanichpaisal, P., B. L. Lee, and K. Söderhäll. 2006. Cell-mediated immunity in arthropods: Hematopoiesis, coagulation, melanization and opsonization. Immunobiology 211: 213–236.

Kanost, M. R., and M. J. Gorman. 2008. Phenoloxidases in insect immunity, pp. 69-96. *In* **N. E. Beckage** (ed.), Insect immunity. Academic Press, San Diego, CA.

Kumar, S., M. Nei, J. Dudley, and K. Tamura. 2008. MEGA: a biologist-centric software for evolutionary analysis of DNA and protein sequences. Brief Bioinform. 9: 299–306.

Lavine, M. D., G. Chen, and M. R. Strand. 2005. Immune challenge differentially affects transcript abundance of three antimicrobial peptides in hemocytes from the moth *Pseudoplusia includens*. Insect Biochem. Mol. Biol. 35: 1335–1346.

Lee, S. Y., M. Y. Cho, J. H. Hyun, K. M. Lee, K. Homma, S. Atori, and S. I. Kawabata. 1998. Molecular cloning of cDNA for pro-phenol-oxidase-activating factor I, a serine protease is induced by lipopolysaccharide or 1,3-β-glucan in coleopteran insect, *Holotrichia diomphalia* larvae. Eur. J. Biochem. 257: 615–621.

Marmaras, V. J., and M. Lampropoulou. 2009. Regulators and signalling in insect haemocyte immunity. Cell. Signal. 21: 186–195.

Nappi, A. J., and E. Ottaviani. 2000. Cytotoxicity and cytotoxic molecules in invertebrates. Bioessays 22: 469–480.

Peirson, S. N., J. N. Butler, and R. G. Foster. 2003. Experimental validation of novel and conventional approaches to quantitative real-time PCR data analysis. Nucleic Acids Res. 31: e73.

Ross, J., H. B. Jiang, M. R. Kanost, and Y. Wang. 2003. Serine proteases and their homologs in the *Drosophila melanogaster* genome: an initial analysis of sequence conservation and phylogenetic relationships. Gene 204: 117–131.

Sarauer, B. L., C. Gillott, and D. Hegedus. 2003. Characterization of an intestinal mucin from the peritrophic matrix of the diamondback moth, *Plutella xylostella*. Insect Mol. Biol. 12: 333–343.

Satoh, D., A. Horii, M. Ochiai, and M. Ashida. 1999. Prophenoloxidase-activating enzyme of the silkworm, *Bombyx mori*: purification, characterization and cDNA cloning. J. Biol. Chem. 274: 7441–7453.

Schuler, T. H., I. Denholm, S. J. Clark, C. N. Stewart, and G. M. Poppy. 2004. Effects of Bt plants on the development and survival of the parasitoid *Cotesia plutellae* (Hymenoptera: Braconidae) in susceptible and Bt-resistant larvae of the diamondback moth, *Plutella xylostella* (Lepidoptera: Plutellidae). J. Insect Physiol. 50: 435–443.

Talekar, N. S., and A. M. Shelton. 1993. Biology, ecology and management of the diamondback moth. Ann. Rev. Entomol. 38: 275–301.

Thompson, J. D., T. J. Gibson, F. Plewniak, F. Jeanmougin, and D. G. Higgins. 1997. The CLUSTAL_X windows interface: flexible strategies for multiple sequence alignment aided by quality analysis tools. Nucleic Acids Res. 25: 4876–4882.

Zou, Z., Y. Wang, and H. B. Jiang. 2005. *Manduca sexta* prophenoloxidae activating proteinase-1 (PAP-1) gene: organization, expression, and regulation by immune and hormonal signals. Insect Biochem. Mol. Biol. 35: 627–636.

Received 4 March 2013; accepted 8 May 2013.